Polymer Bulletin (2023) 80:5417–5431
https://doi.org/10.1007/s00289-022-04346-4

ORIGINAL PAPER

Development and evaluation of antimicrobial LDPE/TiO_2 nanocomposites for food packaging applications

Ahmed M. Youssef[1] · **Mahmoud E. Abd El-Aziz**[2] · **Samir M. M. Morsi**[2]

Received: 23 March 2022 / Revised: 13 June 2022 / Accepted: 14 June 2022 /
Published online: 29 June 2022

Abstract

Polymers used in food packaging should have unique properties, including anti-bacterial properties, good mechanical properties and permeability to air and water. To achieve these properties, some nanomaterials are incorporated into the polymeric matrix to be suitable for such a precise application. Thus, polymer nanocomposites emerged as one of the most important recent trends in the packaging materials industry. Here, titanium dioxide nanoparticles (TiO_2-NPs) were synthesized by the sol–gel method and incorporated into pure low-density polyethylene (P-LDPE) at different concentrations (0, 2, 4, 8 wt %.). The prepared nanocomposites were characterized via a scanning electron microscope (SEM), X-ray diffraction (XRD), and thermogravimetric analysis. The size of TiO_2-NPs is ranged from 13 to 47 nm. The crystallinity index of LDPE increased by the addition of TiO_2-NPs from 0.32 to 0.55. Also, the thermal stability of LDPE improved by 67 °C. Studies of the mechanical properties, antibacterial activity and permeability measurements of nanocomposites films have demonstrated their potential for use in perishable food packaging. The results showed an increase in oxygen permeability from 55.25 cc/M^2 day for P-LDPE to 72.84 cc/M^2 day for LDPE-loaded with 8% TiO_2. On the contrary, the impeded TiO_2-NPs inside LDPE films reduced the water vapor transmission from 2.22 g/(m^2 day) to 0.92 g/(m^2 day). The tensile strength of P-LDPE increased from 16.7 MPa to 28.95 MPa for nanocomposite loaded with 8% TiO_2. The ability of TiO_2-NPs O_2 to generate the potentially reactive radical species induced the antibacterial activity of LDPE to Gram-negative and Gram-positive bacteria.

Keywords Polymer nanocomposites · Nanomaterials · Mechanical properties · Packaging · Antimicrobial activity

✉ Mahmoud E. Abd El-Aziz
Mahmoud_essam12@yahoo.com

[1] Packaging Materials Department, National Research Centre, 33 El-Bohouth St. (Former El-Tahrir St.) Dokki, Giza, Egypt

[2] Polymers and Pigments Department, National Research Centre, 33 El Bohouth St, Dokki, Giza 12622, Egypt

Introduction

The new packaging was considered an effective tool for sustaining the foodstuff quality. It also helps to enhance the values of a product by imparting information and promoting sales [1, 2]. The determinants such as size, safety, price of recyclability, convenience, and packaging are highly significant, as well as design should also be taken into consideration [3]. Commonly, the technologies used to pack foodstuff mainly comprised of air-permeable packaging, modified atmosphere packaging, and vacuum packaging. In the last few years, technological advancements in machinery, methodology, and materials have improved the function and efficiency of foodstuff packaging [4, 5].

The use of antimicrobial either by spraying or dipping the product surface is one of the conventional methods for managing the growth of microbes thereby delaying spoilage and increasing safety [6, 7]. The effectiveness of this application is limited because of the unrestricted movement into the partial and food inactivation of the active compounds. One new strategy to prevent these restrictions is the utilization of antimicrobial packaging methods because it is considered an effective kind of active packaging [8]. In antimicrobial packaging, the incorporation of antimicrobial agencies takes place into the material packaging, covered with the surface of sachet or packaging film [9, 10]. It has been demonstrated in different researches that when antimicrobial agents are incorporated into the packaging films, the levels of foodborne organisms get reduced to significant levels [11, 12]. The incorporation of benzoic anhydride or imazalil in LDPE films can improve the antimicrobial effect of the prepared films [13, 14].

Recently, nanotechnology has evolved the application of food packaging, where manipulation of packaging materials takes place for bringing considerable improvement in biodegradability, heat and mechanical resistance properties, barrier properties, and retardancy of flame in comparison with the normal polymer. It also makes use of different choices for creating antifungal and antimicrobial surfaces and signaling, as well as sensing the biochemical and microbiological changes [15, 16]. Nanotechnology helps to enhance the bioactive nano-materials into the nanocomposite film. A nanocomposite is a kind of solid multiphase substance fortified with fibers, tubes, or particles in a nanometer scale, which eventually provide good chemical and mechanical properties than traditional composites [17, 18]. For example, the nanocomposites could be comprised of a natural or synthetic polymer and inorganic particles in nanoscale such as nano-silver, calcium carbonate, and zinc oxide, as well as carbon-nanotubes [19–22]. Videira-Quintela et al. [23] used silver, copper, and copper hydroxynitrate-fumed silica as reinforced materials for LDPE to prepare packaging films for acidic, alcoholic, and aqueous foodstuffs. Also, Rojas et al. [24] prepared antimicrobial nanocomposites based on LDPE and ZnO-NPs for food packaging.

Titanium dioxide nanoparticles (TiO_2-NPs) are considered the most preferred photocatalyst because of their flair implication in the breakdown of organic pollutants such as pesticides and dyes. Similarly, TiO_2-NPs are believed to be the most appropriate catalyst for environmentally friendly applications because

of their non-toxicity [25–27]. The photocatalytic response of TiO_2-NPs shows increased reliance on the particle's size, surface area, and crystalline structure [19, 28]. The significance of utilizing TiO_2-NPs in material packaging is generally realized through its biological properties and physiochemical feature. The incorporation of TiO_2-NPs with polymers opens the way for the growth of various wrapping materials customized for food packaging purposes [29, 30].

In the existing research, TiO_2-NPs have been prepared; then, it was added to LDPE by different concentrations and inspected the antibacterial, thermal and mechanical activity of the developed LDPE nanocomposites based on TiO_2-NPs.

Materials

Pure low-density polyethylene (P-LDPE) of food grade was purchased from Exxon-Mobil Chemical, Kingdom of Saudi Arabia. The properties of P-LDPE are listed as follow: density ~ 0.93 g/cm^3, melt flow index ~ 6.0 g/10 min/ 190 °C/ 2.16 kg, and softening point ~ 87.4 °C. Titanium (IV) isopropoxide, 97% (TTIP) and nitric acid (HNO_3) were obtained from Sigma-Aldrich chemicals that are used to prepare TiO_2 NPs.

Preparation of titanium dioxide nanoparticles (TiO_2-NPs)

TiO_2-NPs were synthesized by the sol–gel method as described by Youssef et al. [31]. This method depends on the hydrolysis and subsequent condensation processes of titanium tetraisopropoxide (TTIP) as a precursor. Two solutions have been prepared; in the first container, 5 ml TTIP was mixed with 20 ml isopropanol. However, in the second container, distilled water was adjusted at pH 2–3 by using concentrated HNO_3. The second container was dropped wisely added to the other container with continuous stirring at room temperature. After two hours, the temperature was raised to 60–70 °C and kept at this condition for 20 h. The clear transparent sol becomes milky, and finally, the gel was obtained. The latter was subjected to a drying process at 110 °C for 16 h and ground into an agate mortar. Finally, TiO_2-NPs were obtained by the calcination of the ground powder at 550 °C for 2 h.

Preparation of LDPE nanocomposites film

The preparation of nanocomposite films was carried out by melt blending using HAAkE™ Rheomex TW100 Twin-Screw Extruder with 40 cm intermeshing screws. The melt blending was accomplished at 220 °C for 5 min. The sheets of the sample were developed by making use of two heated plates and a hydraulic press (Bucher plastics press KHL 100) 120 bar and at 200 °C. The composition of the prepared nanocomposites is provided in Table 1.

Table 1 The chemical composition of the LDPE nanocomposites films

Sample code	LDPE %	TiO2-NPs %
P-LDPE	100	0
LDPE/ 2% TiO_2-NPs	98	2
LDPE/ 4% TiO_2-NPs	96	4
LDPE/ 8% TiO_2-NPs	92	8

Characterization

X-ray diffraction (XRD)

The nanocomposite films were examined in a Philips PW 1830 diffractometer by XRD through the use of radiation emitting from CuKα (λ = 0.154 nm) at 35 mA and 40 kV. The correctness of dL values determination was carried out at ± 0.01 nm. The degree of crystallinity (CD) is determined by the proposed Segal et al. equation [32]

$$X_c = \frac{A_c}{A_c + A_a} \times 100$$

where A_c and A_a are the area of crystalline and amorphous peaks, respectively.

Thermal analysis

Thermogravimetric analysis was carried out by using the tool of Mettler-Toledo TGA/SDTA 851^e with a heating rate of 5 °C/min and at air atmosphere. The measurements of differential scanning calorimetry (DSC) were carried out in the specific range of temperature at 25–200 °C at 5 °C/min heating rate under nitrogen atmosphere. The tested samples were first heated to 200 °C to completely melt and eliminate the influence of thermal history and then cooled to 25 °C to obtain a crystallization process curve.

Crystallinity (X_c) is calculated from the following equation

$$X_c = \frac{\Delta H_m}{\Delta H_{100}} \times 100$$

where ΔH_m is the enthalpy of the sample melting endotherm, while ΔH_{100} is the melting enthalpy of 100% crystalline LDPE [33].

Electron microscope

High-Resolution Quanta FEG 250-SEM Scanning Electron Microscope, Czech Republic, was used to study the surface morphology of the prepared TiO_2–NPs. The shape and size of TiO_2–NPs were detected by JEOL-2100 Transmission Electron Microscope (TEM) operated at 80 kV. The mechanical properties of P-LDPE and nanocomposites

sheets, such as tensile strength and elongation at break, were studied by cutting them in dumbbell shapes and tested with a universal testing machine LK10k installed with a 5 kN load cell. Three measurements were performed for each sample according to ASTM D638-91.

Water vapor and oxygen permeability measurements

Water vapor transmission rate (WVTR) was determined by the Water Vapor Permeability Analyzer (GBI W303 (B), China) through the cup method. WVTR was computed by calculating the mass of water vapor passing per unit time through a unit area and under a controlled humidity (4%) and temperature (38 °C). This method is stated by the standards JIS Z0208, DIN 53,122–1, TAPPI T464, ASTM D1653, ISO 2528 and ATM E96.

The oxygen gas transmission rate (OTR) for pure P-LDPE and LDPE/TiO_2-NP nanocomposites was computed via means of an N530 Gas Permeability Analyzer (China) in accordance with the standards ASTM D1434-82 (reapproved 2015), GB/T 1038–2000, and ISO 2556–2001. For both WVTR and OTR measurements, the apparatus used smooth and uniform plastic films with thickness of 200 mm. The evaluation test was repeated three times, and the average values were recorded.

Antimicrobial activity measurements

Antibacterial activities of P-LDPE and nanocomposites against gram-negative bacteria (G^-) as *Pseudomonas aeruginosa* ATCC 27853 and gram-positive bacteria (G^+) as *Staphylococcus aureus* ATCC6538-P were determined using modified Kirby–Bauer disk diffusion method by Hioki 3522-50 LCR Hitester (Japan). Mueller–Hinton agar was used for determination of susceptibility of microorganisms to antimicrobial agents. Measurements were carried out at "Microbiological Department, National Research Centre.

Results and discussion

TEM and SEM images of the prepared TiO_2-NPs

Figure 1a and b shows the TEM and SEM images of the prepared TiO_2-NPs, respectively. TEM image of TiO_2-NPs (Fig. 1a) shows different shapes of titanium particles from spherical particles to rounded-corners polygons. The particle diameter ranges from 13 to 47 nm revealing the nanoscale of these particles. The morphological structure of the titanium particles is shown in Fig. 1b. The majority of the particles are spherical in shape, while some other irregular shapes also appear.

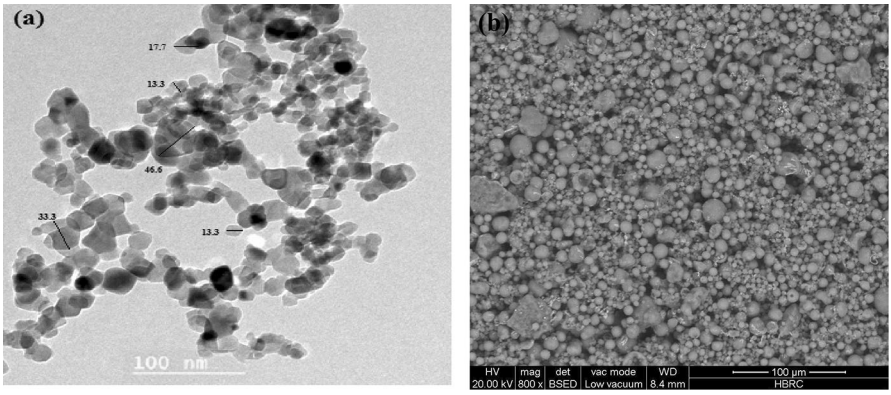

Fig. 1 TEM (**a**) and SEM (**b**) images of TiO_2-NPs

Characterizations of the prepared nanocomposites

SEM and EDX analysis

Figure 2a and b shows the SEM surface images of P-LDPE and LDPE/8% TiO_2-NPs films, respectively. The SEM micrograph of the P-LDPE film shows a uniform continuous matrix with a smooth surface. However, the addition of TiO_2-NPs did not show any kind of phase separation between the dispersed particles and the LDPE matrix. This indicates the success of the blending process and the dispersion of the TiO_2-NPs in the LDPE polymeric matrix.

Figure 2a inset and b inset shows the EDX spectra of P-LDPE and LDPE/8%TiO_2-NPs nanocomposite, respectively. The EDX profile of P-LDPE exhibited the emergence of two peaks. The first is a strong energy peak at 0.23 keV related to K-shell electron of LDPE carbon atoms. However, the second very small peak at 0.5 keV is related to K-shell electron of oxygen atoms of some additives in the LDPE. It can be seen that the intensity of this peak increased significantly in the EDX profile of LDPE/8%TiO_2-NPs nanocomposite. Two other new peaks in the range from 4.5 keV to 5 keV are related to the K_α and K_β electrons of Ti atoms. This spectrum pattern indicates the embedding of TiO_2-NPs within the LDPE matrix.

XRD analysis

X-ray diffraction (XRD) patterns of the synthesized TiO_2-NPs, P-LDPE, LDPE/2%TiO_2-NPs nanocomposite, and LDPE/8%TiO_2-NPs nanocomposite are shown in Fig. 3. It can observed from Fig. 3a that the peaks of the prepared TiO_2-NPs are emerged at $2\Theta \approx 25.21°$, 37.28°, 47.99°, 53.95°, 55.1°, 62.65°, 69.47° and 75.38° which assigns to (101), (004), (200), (105), (211), (204), (220) and (215) planes, respectively. This diffraction pattern is in a good agreement with the reference anatase TiO_2 (JCPDS No. 21-1272). The anatase major phase

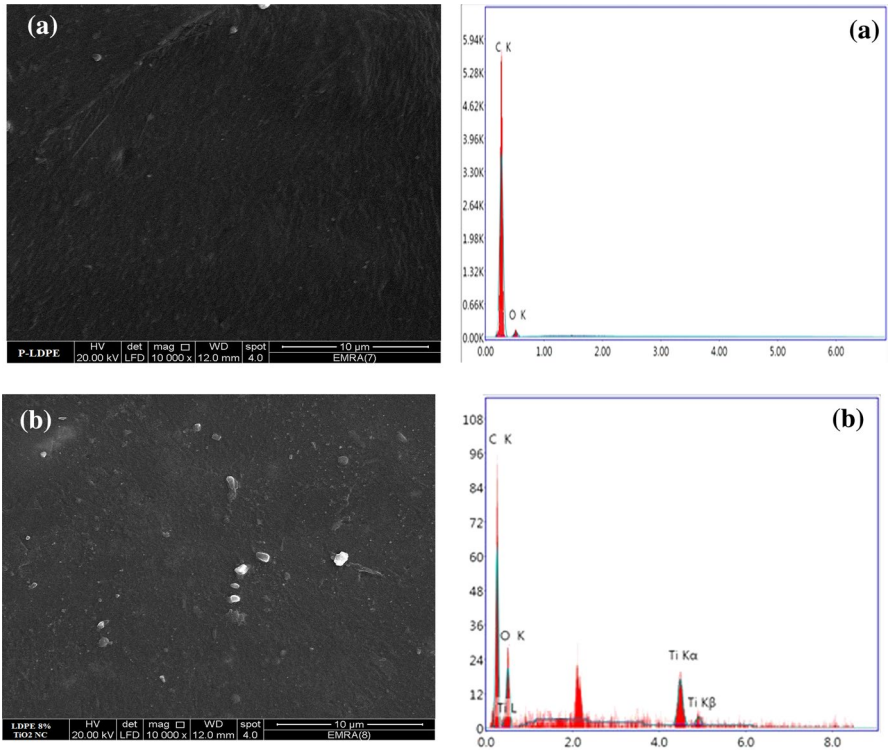

Fig. 2 SEM surface images and EDX spectra of **a** P-LDPE and **b** LDPE/8%TiO_2-NPs nanocomposite

of tetragonal structure can be confirmed by the strong diffraction peaks at 25.21° and 47.99°. However, the presence of some rutile type can be proved by the diffraction peaks at 27.11° and 35.5° of (110) and (101) planes. The XRD diffraction pattern of P-LDPE (Fig. 3b) shows two crystalline peaks at Bragg angles of $2\theta \approx 21.56°$ (110) and 23.38 (200) which is in a good agreement with the reference polyethylene (JSPDS card 11-0834). The XRD pattern reflects the semi-crystalline structure of P-LDPE where the polymer matrix is a mixture of crystalline and amorphous regions. The deconvolution method was used to separate the two regions, and the degree of crystallinity was estimated to be 31.86%.

However, for the nanocomposites (Fig. 3c and d), the insertion of TiO_2-NPs led to shift 110 and 200 planes diffraction peak of LDPE to higher values. 110 plane is shifted to $2\theta \approx 21.58°$ and 21.61°, respectively. Also, 200 plane is shifted to 23.71° and 23.99°, respectively. The diffraction peak of anatase TiO_2 emerges as a small hump at 25.11°–25.40° in the two nanocomposites XRD spectra. However, the intensity of this peak is greater in the nanocomposite of LDPE/8% TiO_2-NPs than LDPE/2% TiO_2-NPs indicating an increased amount of TiO_2-NPs embedded in the polyethylene matrix. Loading of LDPE with TiO_2-NPs increased the

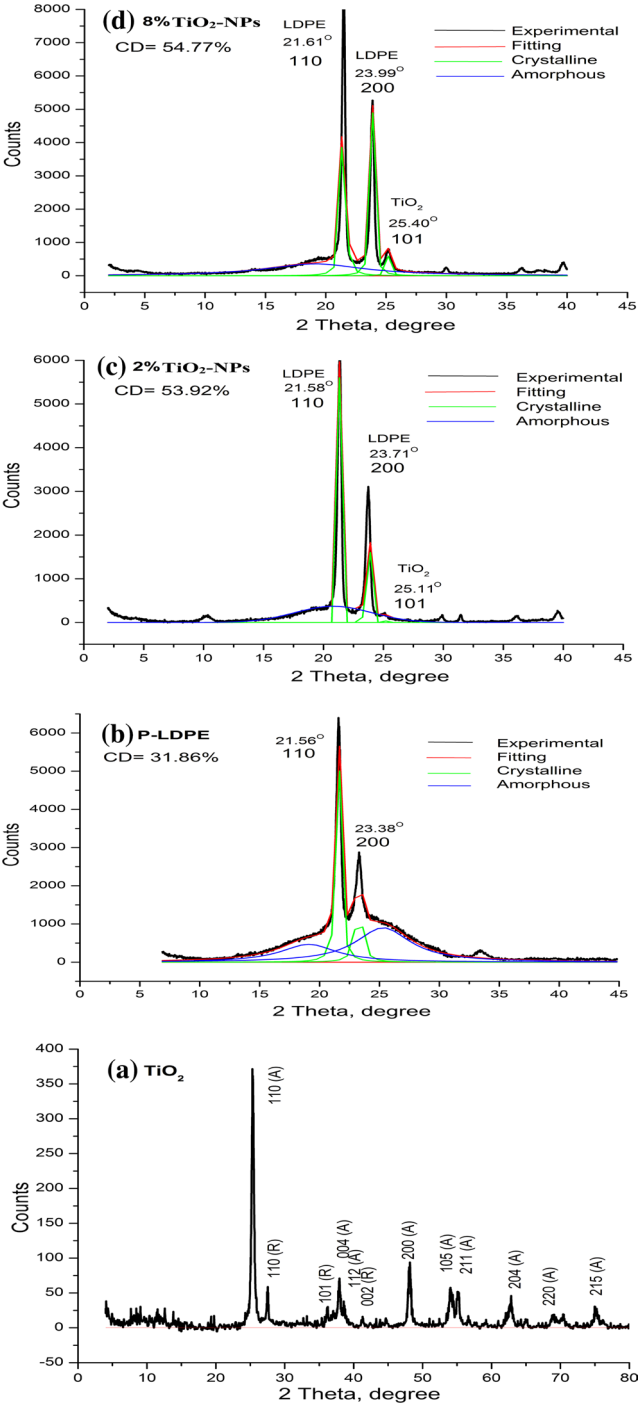

Fig. 3 XRD of **a** TiO_2-NPs, **b** P-LDPE, **c** LDPE/2%TiO_2–NPs and **d** LDPE/8%TiO_2–NPs

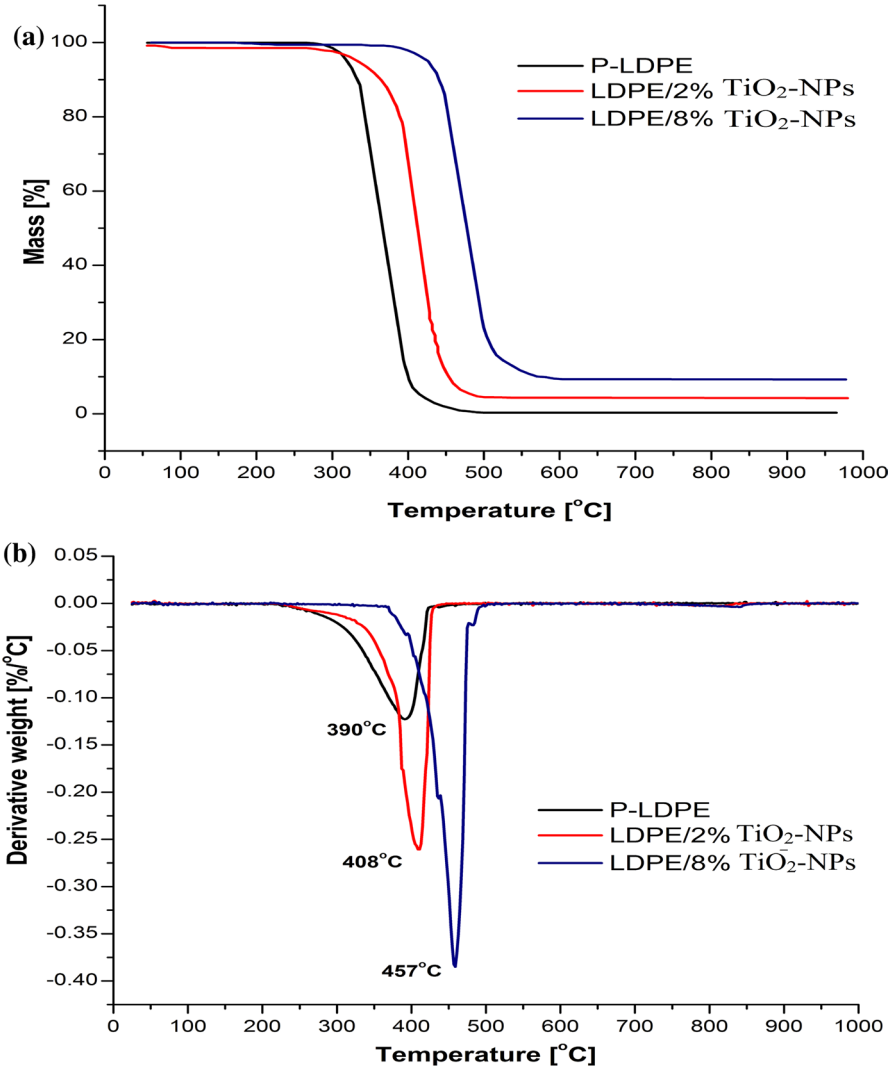

Fig. 4 TGA (**a**) and DTG (**b**) curves of P-LDPE, LDPE/2%TiO_2-NPs and LDPE/8% TiO_2-NPs

crystallization regions in the nanocomposite matrix to 53.92% for LDPE/2%TiO_2-NPs and 54.77% for LDPE/8%TiO_2-NPs.

Thermal properties of the prepared nanocomposites

The thermal degradation of pure LDPE and the prepared LDPE/2%TiO_2-NPs and LDPE/8%TiO_2-NPs is presented in Fig. 4a. The TGA curve of pure LDPE shows one stage of degradation from around 300 °C to 420 °C, in which complete mass loss occurred. This degradation step is due to the depolymerization of

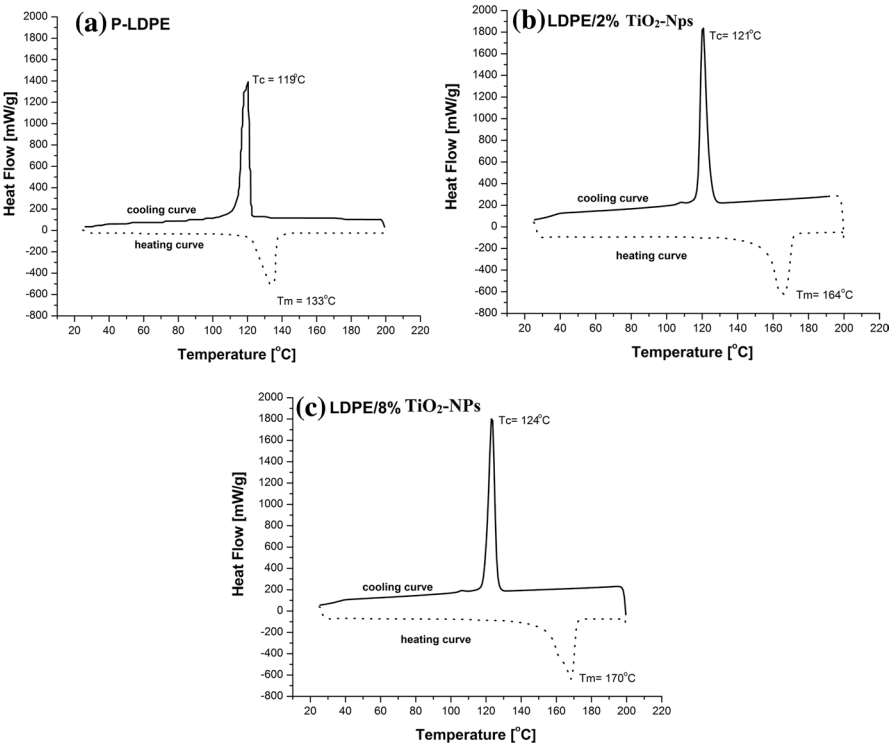

Fig. 5 DSC curves of **a** P-LDPE, **b** LDPE/2% TiO_2-NPs, and **c** LDPE/8% TiO_2-NPs

polyethylene chains at the weak C–C sites. The results of this thermo-degradation process are gaseous products. However, the addition of TiO_2-NPs to the LDPE matrix increased the thermal stability of the nanocomposites, where the thermal decomposition of both LDPE/2% TiO_2-NPs and LDPE/8% TiO_2-NPs begins at about 330 °C and 420 °C, respectively. Thus, the increase in the amount of titanium particles led to an increase in the thermal stability of the LDPE. This may be attributed to some physical interactions formed between polyethylene chains and the TiO_2-NPs. Furthermore, the mass loss at the decomposition step of the nanocomposites is not as complete as that of P-LDPE. This is due to the remnants of titania particles which is higher in LDPE/8%TiO_2-NPs (≈ 9%) than in LDPE/2%TiO_2-NPs (≈ 4%).

The DTG curves of P-LDPE and the fabricated nanocomposite are displayed in Fig. 4b. The curves clarify the higher thermal stability obtained by incorporating titanium particles into the polyethylene matrix. The maximum decomposition temperature of P-LDPE was obtained at 390 °C, which was upgraded by adding 2% and 8% TiO_2-NPs to 408 °C and 457 °C, respectively. This can be attributed to the hypothetical that the TiO_2-NPs have involved in physical interactions with LDPE matrix, which requires a higher thermal energy to break these interactions.

Table 2 The OTR and WVTR for the prepared LDPE nanocomposites

Samples	OTR (cc/m^2 day)	WVTR g/(m^2 day)
P-LDPE	55. 25 ± 3.3	2.22 ± 0.9
LDPE/ 2% TiO_2-NPs	60.87 ± 3.8	1.94 ± 0.9
LDPE/ 4% TiO_2-NPs	68.34 ± 4.2	1.35 ± 0.7
LDPE/ 8% TiO_2-NPs	72.84 ± 4.0	0.92 ± 0.55

The DSC measurements are illustrated in Fig. 5. The heating DSC curve shows the melting temperature of the samples. P-LDPE showed a melting endotherm at 133 °C, while the heat of melting was greatly increased by adding TiO_2-NPs to the LDPE matrix to 164 °C in LDPE/2% TiO_2-NPs and 170 °C in LDPE/8% TiO_2-NPs. The crystallinity of the samples was determined from the heat enthalpy of the melt endothermic peaks to be 35.35% for P-LDPE, 51.54% for LDPE/2% TiO_2-NPs, and 51.92% for LDPE/8% TiO_2-NPs. These values are close to that obtained from the XRD analysis. The crystallization temperatures of the samples can be detected from the cooling curves. P-LDPE, LDPE/2% TiO_2-NPs, and LDPE/8% TiO_2-NPs cooling curves showed exothermic peaks at 119 °C, 121 °C, and 124 °C, respectively. This gradual increase in the crystallization temperature as well as the melting temperature proves the physical interactions generated by TiO_2-NPs with the polyethylene matrix.

Oxygen and moisture permeability of the papered LDPE nanocomposites

The oxygen transmission rate (OTR) and water vapor transmission rate (WVTR) are important factors of the packaging materials to determine their protection barrier properties. Table 2 illustrates the WVTR and OTR of P-LDPE and the fabricated nanocomposite films. It has been demonstrated through the data collected from the WVTR toll that nanocomposite films of LDPE/TiO_2 have low WVTR compared to the P-LDPE. By increasing the loadings of TiO_2-NPs in the fabricated nanocomposites of LDPE/TiO_2, a significant decrease has occurred in the values of WVTR. The addition of TiO_2-NPs with 2, 4, and 8 wt% reduced the WVTR film's value to 0.92, 1.35, and 1.94 g/(m^2.24 h), respectively, in comparison with 2.22 g/(m^2 day) for P-LDPE. The mechanism of transmitting the water vapors can be elaborated as the number of transmission phases in which the water first liquefies and condenses on the prepared surface of nanocomposites films followed by the liquid water transmission across the film and the complete water vapor evaporation from the other film's side. TiO_2-NPs created a "tortuous path" in the LDPE for gas molecules to traverse the nanocomposite barrier and decreased the porosity that formed in LDPE film. Therefore, the filling titania nanoparticles inside LDPE enhance the barrier properties of the produced nanocomposites and decrease the transmission rate of water vapor [34–36]. Thus, these nanocomposites can become an optimum choice for high barrier packaging films.

However, an increase in OTR occurred by loading the TiO_2-NPs in the matrix of LDPE as illustrated in (Table 2). The OTR for LDPE is 55.25 (cc/M^2 day) which

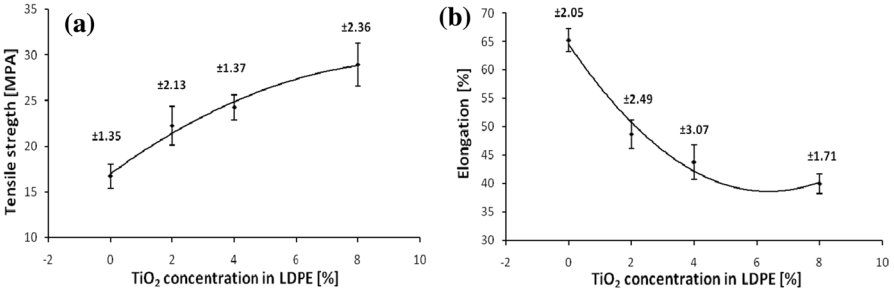

Fig. 6 Tensile strength (**a**) and elongation (**b**) of P-LDPE, LDPE/2% TiO_2-NPs, LDPE/4% TiO_2-NPs and LDPE/8% TiO_2-NPs

is enhanced by the addition of TiO_2-NPs and increased by increasing the addition ratios (2, 4, and 8%) of TiO_2-NPs to be 60.87, 68.34, and 72.84 (cc/M^2 day), respectively. That means the prepared LDPE/TiO_2 nanocomposites become suitable for use as packaging materials for different food products.

Mechanical properties of the prepared LDPE nanocomposites

Figure 6 lists the tensile strength and elongation at break measurements of the prepared materials, which express the effect of TiO_2-NPs on the mechanical properties of LDPE. It is clear that in the range from 0 to 8% TiO_2-NPs, the tensile strength shows an increasing tendency in its values, while the elongation at break declines. The tensile strength increased from 16.7 MPa for P-LDPE to a maximum of 28.95 MPa for LDPE/8% TiO_2-NPs. This behavior can be attributed to the fact that the addition of nanoscale materials to the polymer changes the mechanical properties of the polymeric matrix. The titanium particles participated in physical interactions with the polyethylene chains, which led to a continuous increase in the tensile strength and a decrease in elongation with the increasing the amount of titanium particles in the matrix. However, the persistence of this mechanical behavior even at high amounts of titanium, which reaches 8%, indicates the perfect distribution of TiO_2-NPs and the absence of agglomerations within LDPE matrix.

Antibacterial activity of the prepared nanocomposites

The antibacterial activity of P-LDPE and the prepared nanocomposites was conducted by the disk diffusion procedure, as described by Youssef et al. [25], to assess the effect of TiO_2-NPs on the LDPE. The tests were examined against Gram-negative (*Pseudomonas aeruginosa*) and Gram-positive bacteria (*Staphylococcus aureus*), and the results are listed in Table 3. As clear, there is no antibacterial effect of P-LDPE on both Gram-negative and Gram-positive bacteria. However, the addition of TiO_2-NPs led to the acquisition of LDPE to an activity against bacterial cells. This antibacterial activity increased with increasing the amount of titania in the LDPE matrix. TiO_2-NPs have the ability to produce reactive oxygen species when exposed to sunlight such as hydrogen peroxide, superoxide radical, hydroxyl

Table 3 The clear inhibition zone of the prepared LDPE nanocomposites

Samples	Clear inhibition zone (θmm)	
	Staphylococcus aureus	*Pseudomonas aeruginosa*
P-LDPE	0.0	0.0
LDPE/2% TiO_2-NPs	16	18
LDPE/4% TiO_2-NPs	16	19
LDPE/8% TiO_2-NPs	18	20

radical and singlet oxygen. These species are highly effective against Gram-positive and Gram-negative bacteria [37]. Therefore, the photocatalytic effect and the specific hydrophilic properties of TiO_2-NPs caused the antimicrobial protecting characteristics of the nanocomposites. Moreover, the efficiency is slightly more against *Pseudomonas aeruginosa* than against *Staphylococcus aureus*. This can be attributed to that the polar hydrophilic titania particles and the reactive species can diffuse more easily through the negatively charged lipopolysaccharide outer membrane of *Pseudomonas aeruginosa* than the thick peptidoglycan cell wall of *Staphylococcus aureus*. The reactive species destroy the outer membrane of the bacteria and finally damage the bacteria.

Conclusion

TiO_2-NPs were prepared by sol–gel method and incorporated into low-density polyethylene matrices with the target of using the resulting nanocomposites as food packaging materials. The results of XRD showed that the TiO_2-NPs increased the crystallinity of the polyethylene matrix by 69% to 72%. The mechanical properties of P-LDPE were improved to the maximum by adding 8% TiO_2-NPs, as the tensile strength of the nanocomposites increased by 73%. The maximum decomposition temperature of the polyethylene increased from 390 °C to 457 °C by introducing 8% TiO_2-NPs indicating an improvement in the thermal stability of the nanocomposites. Polyethylene has gained antibacterial activity by adding TiO_2-NPs due to their photocatalytic properties which enable them to produce reactive species. The latter have high antibacterial effect against Gram-positive and Gram-negative bacteria. The oxygen permeability increased and water vapor transmission decreased by the addition of TiO_2-NPs inside LDPE films. These results prove that the prepared nanocomposites can be used as packaging materials for food.

References

1. Ghaani M, Cozzolino CA, Castelli G, Farris S (2016) An overview of the intelligent packaging technologies in the food sector. Trends Food Sci Technol 51:1–11. https://doi.org/10.1016/j.tifs.2016.02.008

2. Youssef AM, Bujdosó T, Hornok V, Papp S, Dékány I (2013) Structural and thermal properties of polystyrene nanocomposites containing hydrophilic and hydrophobic layered double hydroxides. Appl Clay Sci 77:46–51
3. Duizer LM, Robertson T, Han J (2009) Requirements for packaging from an ageing consumer's perspective. Packag Technol Sci 22(4):187–197. https://doi.org/10.1002/pts.834
4. Nollet LM, Toldrá F (2006) Advanced technologies for meat processing, CRC Press
5. Youssef AM (2013) Polymer nanocomposites as a new trend for packaging applications. Polym-Plast Technol Eng 52(7):635–660. https://doi.org/10.1080/03602559.2012.762673
6. Kerry JP, O'Grady MN, Hogan SA (2006) Past, current and potential utilisation of active and intelligent packaging systems for meat and muscle-based products: a review. Meat Sci 74(1):113–130. https://doi.org/10.1016/j.meatsci.2006.04.024
7. El-Mohamedy R, Abd El-Aziz ME, Kamel S (2019) Antifungal activity of chitosan nanoparticles against some plant pathogenic fungi in vitro. Agric Eng Int CIGR J 21(4):201–209
8. El-Wakil AE-AA, Moustafa H, Youssef AM (2020) Antimicrobial low-density polyethylene/low-density polyethylene-grafted acrylic acid biocomposites based on rice bran with tea tree oil for food packaging applications. J Thermoplast Compos Mater 35(7):938–956. https://doi.org/10.1177/0892705720925140
9. Devlieghere F, Vermeiren L, Debevere J (2004) New preservation technologies: possibilities and limitations. Int Dairy J 14(4):273–285. https://doi.org/10.1016/j.idairyj.2003.07.002
10. Hong S-I, Rhim J-W (2008) Antimicrobial activity of organically modified nano-clays. J Nanosci Nanotechnol 8(11):5818–5824. https://doi.org/10.1166/jnn.2008.248
11. Hassan B, Chatha SAS, Hussain AI, Zia KM, Akhtar N (2018) Recent advances on polysaccharides, lipids and protein based edible films and coatings: a review. Int J Biol Macromol 109:1095–1107. https://doi.org/10.1016/j.ijbiomac.2017.11.097
12. Youssef A, Abd El-Aziz M, El-Sayed E, Abdel-Aziz M, El-Hakim AA, Kamel S, Turky G (2018) Morphological, electrical & antibacterial properties of trilayered Cs/PAA/PPy bionanocomposites hydrogel based on Fe_3O_4-NPs. Carbohyd Polym 196:483–493
13. Corrales M, Fernández A, Han JH (2014) Chapter 7—antimicrobial packaging systems. In: Han JH (ed) Innovations in food packaging (second edition). Academic Press, San Diego, pp 133–170
14. Suppakul P, Miltz J, Sonneveld K, Bigger SW (2003) Active packaging technologies with an emphasis on antimicrobial packaging and its applications. J Food Sci 68(2):408–420. https://doi.org/10.1111/j.1365-2621.2003.tb05687.x
15. Chau C-F, Wu S-H, Yen G-C (2007) The development of regulations for food nanotechnology. Trends Food Sci Technol 18(5):269–280. https://doi.org/10.1016/j.tifs.2007.01.007
16. Amna T, Yang J, Ryu K-S, Hwang IH (2015) Electrospun antimicrobial hybrid mats: Innovative packaging material for meat and meat-products. J Food Sci Technol 52(7):4600–4606. https://doi.org/10.1007/s13197-014-1508-2
17. Sharma B, Malik P, Jain P (2018) Biopolymer reinforced nanocomposites: a comprehensive review. Mater Today Commun 16:353–363. https://doi.org/10.1016/j.mtcomm.2018.07.004
18. Fernández MJ, Fernández MD (2020) Effect of organic modifier and clay content on non-isothermal cold crystallization and melting behavior of polylactide/organovermiculite. Nanocompos Polym 12(2). https://doi.org/10.3390/polym12020364
19. Youssef AM, Hasanin MS, Abd El-Aziz ME, Turky GM (2021) Conducting chitosan/hydroxylethyl cellulose/polyaniline bionanocomposites hydrogel based on graphene oxide doped with Ag-NPs. Int J Biol Macromol 167:1435–1444. https://doi.org/10.1016/j.ijbiomac.2020.11.097
20. Cai G-B, Zhao G-X, Wang X-K, Yu S-H (2010) Synthesis of polyacrylic acid stabilized amorphous calcium carbonate nanoparticles and their application for removal of toxic heavy metal ions in water. J Phys Chem C 114(30):12948–12954. https://doi.org/10.1021/jp103464p
21. Chand S (2000) Review carbon fibers for composites. J Mater Sci 35(6):1303–1313. https://doi.org/10.1023/A:1004780301489
22. Youssef AM, El-Sayed SM, El-Sayed HS, Salama HH, Dufresne A (2016) Enhancement of Egyptian soft white cheese shelf life using a novel chitosan/carboxymethyl cellulose/zinc oxide bionanocomposite film. Carbohyd Polym 151:9–19
23. Videira-Quintela D, Guillén F, Martin O, Montalvo G (2022) Antibacterial LDPE films for food packaging application filled with metal-fumed silica dual-side fillers. Food Packag Shelf Life 31:100772. https://doi.org/10.1016/j.fpsl.2021.100772
24. Rojas K, Canales D, Amigo N, Montoille L, Cament A, Rivas LM, Gil-Castell O, Reyes P, Ulloa MT, Ribes-Greus A, Zapata PA (2019) Effective antimicrobial materials based on low-density

polyethylene (LDPE) with zinc oxide (ZnO) nanoparticles. Compos B Eng 172:173–178. https://doi.org/10.1016/j.compositesb.2019.05.054
25. El-Naggar ME, Hasanin M, Youssef AM, Aldalbahi A, El-Newehy MH, Abdelhameed RM (2020) Hydroxyethyl cellulose/bacterial cellulose cryogel dopped silver@titanium oxide nanoparticles: Antimicrobial activity and controlled release of Tebuconazole fungicide. Int J Biol Macromol 165:1010–1021. https://doi.org/10.1016/j.ijbiomac.2020.09.226
26. Dumitriu C, Constantinescu A, Pirvu C (2021) Functionalized TiO_2 nanotube platform for gliadin electroanalysis. Crystals 11(1). https://doi.org/10.3390/cryst11010022
27. El-Maghrabi HH, Barhoum A, Nada AA, Moustafa YM, Seliman SM, Youssef AM, Bechelany M (2018) Synthesis of mesoporous core-shell CdS@TiO2 (0D and 1D) photocatalysts for solar-driven hydrogen fuel production. J Photochem Photobiol A 351:261–270. https://doi.org/10.1016/j.jphotochem.2017.10.048
28. Sobana N, Muruganadham M, Swaminathan M (2006) Nano-Ag particles doped TiO2 for efficient photodegradation of Direct azo dyes. J Mol Catal A: Chem 258(1):124–132. https://doi.org/10.1016/j.molcata.2006.05.013
29. Youssef AM, Malhat FM, Abd El-Hakim AFA (2013) Preparation and utilization of polystyrene nanocomposites based on TiO2 nanowires. Polym Plastics Technol Eng 52(3):228–235. https://doi.org/10.1080/03602559.2012.735311
30. Athir N, Shah SAA, Shehzad FK, Cheng J, Zhang J, Shi L (2020) Rutile TiO2 integrated zwitterion polyurethane composite films as an efficient photostable food packaging material. React Funct Polym 157:104733. https://doi.org/10.1016/j.reactfunctpolym.2020.104733
31. Youssef AM, Assem FM, Abdel-Aziz ME, Elaaser M, Ibrahim OA, Mahmoud M, Abd El-Salam MH (2019) Development of bionanocomposite materials and its use in coating of Ras cheese. Food Chem 270:467–475. https://doi.org/10.1016/j.foodchem.2018.07.114
32. Segal L, Creely JJ, Martin AE, Conrad CM (1959) An empirical method for estimating the degree of crystallinity of native cellulose using the X-ray diffractometer. Text Res J 29(10):786–794. https://doi.org/10.1177/004051755902901003
33. Li D, Zhou L, Wang X, He L, Yang X (2019) Effect of crystallinity of polyethylene with different densities on breakdown strength and conductance property. Materials 12(11). https://doi.org/10.3390/ma12111746
34. Dirim SN, Özden HÖ, Bayındırlı A, Esin A (2004) Modification of water vapour transfer rate of low density polyethylene films for food packaging. J Food Eng 63(1):9–13. https://doi.org/10.1016/S0260-8774(03)00276-0
35. Polat S, Fenercioğlu H, Güçlü M (2018) Effects of metal nanoparticles on the physical and migration properties of low density polyethylene films. J Food Eng 229:32–42. https://doi.org/10.1016/j.jfoodeng.2017.12.004
36. Son S, An J, Choi J, Lee J (2021) Fabrication of TiO2-embedded polyimide layer with high transmittance and improved reliability for liquid crystal displays 13(3):376. https://doi.org/10.3390/polym13030376
37. Dryden M (2018) Reactive oxygen species: a novel antimicrobial. Int J Antimicrob Agents 51(3):299–303. https://doi.org/10.1016/j.ijantimicag.2017.08.029